

Wind-Driven Optimization Technique for Estimation of Solar Photovoltaic Parameters

Derick Mathew¹, Chinnappa Rani¹, *Senior Member, IEEE*, Muthu Rajesh Kumar, *Senior Member, IEEE*, Yue Wang, Richard Binns², and Krishna Busawon², *Senior Member, IEEE*

Abstract—In order to increase the efficiency of the solar photovoltaic (PV) system, accurate electrical modeling of the system under different environmental conditions is necessary. The double-diode electrical model of solar PV is known to be more accurate than its single diode model counterpart since it takes into account the effect of recombination. However, because of its nonlinear characteristics, the parameters of the double-diode model (DDM) have to be identified using optimization algorithms. In this paper, the wind-driven optimization (WDO) algorithm is proposed as a potential new method for identifying the parameters of a 12-parameter DDM of the solar PV. The accuracy and flexibility of the proposed method are verified using three different sets of data: first, experimental data at the controlled environmental condition; second, data sheet values of different solar PV modules; and third, real-time experimental data at the uncontrolled environmental condition. Additionally, the performance of the WDO is compared with other well-known existing optimization techniques. The obtained results show that the WDO algorithm can provide optimized values with reduced mean absolute error in power and reduced root mean square error for different types of solar PV modules at different environmental conditions. We show that the WDO can be confidently recommended as a reliable optimization algorithm for parameter estimation of solar PV model.

Index Terms—Adaptive electrical model, mean absolute error in power (MAEP), parameter estimation, root mean square error (RMSE), wind-driven optimization (WDO).

I. INTRODUCTION

TODAY, due to the continuous decline of conventional fuel sources and their adverse effects of climate change, the use of renewable and inexhaustible energy sources is gradually increasing. Among them, solar energy has emerged as potential alternative to overcome the decline in fossil fuel sources. Large-scale photovoltaic (PV) plants are now commonly used for power generation in most part of the continents. With regards to its practical implementation, the solar PV system should be optimized before its installation. This can be assured by precise

modeling, identification, and simulation of solar PV module. The modeling of solar PV is generally done to describe its current–voltage (I – V) and power–voltage (P – V) relations over a wide range of temperatures and solar irradiances. The I – V relations of solar PVs are usually described using two types of diode models: single diode model and double-diode model (DDM) [1]–[4].

Generally, the unknown parameters of diode models are estimated using curve fitting and optimization techniques. One of the pitfalls of the curve fitting technique is that the parameters are identified only at standard condition. In order to that, different environmental condition requires different sets of parameters to model solar PV. This is because parameters obtained are based on mathematical equations, not on physical interpretation [5]. The parameters of solar PV vary because of the variations in the environmental conditions [5]. Consequently, in this paper, an adaptive electrical model of solar PV in which all the parameters depend on temperature and irradiance has been employed. This, however, leads to extra parameters that need to be identified. More precisely, 12 parameters (12p) for the DDMs. In addition, the parameter estimation procedure has to be carried out only once for all environmental condition because of the adaptive nature of the model.

The next step after modeling the solar PV is the parameter estimation for the model. The popular approaches employed for parameter estimation can be broadly categorized into three main techniques, namely analytical techniques [6], numerical extraction [7], and evolutionary algorithm techniques. Evolutionary algorithm techniques are considered to be excellent in dealing with nonlinear equations. In the recent years, different optimization techniques have been introduced to estimate the parameters of solar PV, namely the genetic algorithm [8], pattern search optimization [9], artificial immune system [10], bacterial foraging algorithm [11], simulated annealing [12], harmony search algorithm [13], artificial bee colony optimization [14], flower pollination algorithm (FPA) [15], and cuckoo search [16]. However, these algorithms still need some modifications to find the most optimized parameters of PV modules [15]. There is, therefore, a real incentive in deriving more efficient algorithms for finding optimized values of parameters of solar PV.

In this paper, we use a new optimization technique called wind-driven optimization (WDO) algorithm for solar PV parameter estimation. The WDO algorithm is developed by Zikri Bayraktar for electromagnetics application [17]. It is a population-based heuristic global optimization technique for

Manuscript received August 28, 2017; revised October 3, 2017; accepted October 17, 2017. Date of publication December 7, 2017; date of current version December 20, 2017. (*Corresponding author: Chinnappa Rani.*)

M. Derick, C. Rani, and M. Rajesh Kumar are with the School of Electrical Engineering, VIT University, Vellore 632014, India (e-mail: derick.mathew@vit.ac.in; crani@vit.ac.in; mrjeshkumar@vit.ac.in).

Y. Wang, R. Binns, and K. Busawon are with the Faculty of Engineering and Environment, Northumbria University, Newcastle upon Tyne NE1 8ST, U.K. (e-mail: yue5.wang@northumbria.ac.uk; Richard.binns@northumbria.ac.uk; krishna.busawon@northumbria.ac.uk).

Color versions of one or more of the figures in this paper are available online at <http://ieeexplore.ieee.org>.

Digital Object Identifier 10.1109/JPHOTOV.2017.2769000

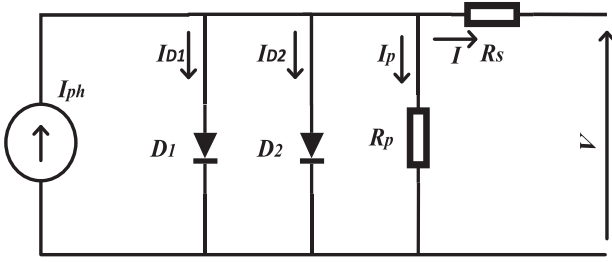


Fig. 1. Double-diode solar PV equivalent circuit.

multidimensional problems. The motivation for WDO algorithm was based on the motion of microscopic air parcels in a multi-dimensional space. The algorithm contains four constants. The optimized values of these constants are generated using covariance matrix adaptation evolution strategy (CMAES) [18].

We employ the WDO algorithm to find optimized values of 12p-DDM adaptive models of solar PV. The accuracy and flexibility of the WDO are verified using three different sets of data, which are as follows:

- 1) experimental data at the controlled environmental condition;
- 2) data sheet values of different solar PV modules; and
- 3) real-time experimental data at the uncontrolled environmental condition.

Additionally, the performance of the WDO is compared with other well-known existing optimization techniques. The results obtained are compared with results presented in the recent literature in order to validate the WDO optimization technique. The obtained results show that the WDO algorithm can provide optimized values with reduced mean absolute error in power (MAEP) and reduced normalized root mean square error (NRMSE) for different types of solar PV. We show that the WDO can be confidently recommended as a reliable optimization algorithm for parameter estimation of solar PV model.

II. MATHEMATICAL MODELING

A. 12-Parameter Double-Diode Model

The DDM is the accurate diode model of solar PV that takes into account the effect of recombination by introducing another diode in parallel to the photon current source. The equivalent circuit of DDM is shown in Fig. 1.

The I - V relation of the DDM of the PV module is represented as

$$I = I_{ph} - I_{o1} \left(e^{\frac{V + I R_s}{N_s V_{t1}}} - 1 \right) - I_{o2} \left(e^{\frac{V + I R_s}{N_s V_{t2}}} - 1 \right) - \frac{V + I R_s}{R_p}. \quad (1)$$

Here, I represents the solar PV current, I_{ph} is the photon current generated by the incident light, I_{o1} and I_{o2} are the reverse saturation current, R_p is the parallel resistance, which accounts for the voltage drops and internal losses because of the flow of current, R_s is the series resistance, which accounts for the leakage current to the ground when diode is in reverse biased, N_s is number of cells connected in series, and V_{t1} and

V_{t2} are thermal voltage, which are represented by

$$V_{t1} = a_1 \frac{KT}{q}, \quad V_{t2} = a_2 \frac{KT}{q}. \quad (2)$$

The values of I_{ph} , I_{o1} , I_{o2} , R_s , and R_p are the important parameters in the diode model. All these parameters depend on the solar irradiance (G) and the temperature (T) [19], [20]. The photon current and reverse saturation currents can be expressed as

$$I_{ph} = \frac{G}{G_{STC}} [I_{phref} + k_i (T - T_{STC})] \quad (3)$$

$$I_o = I_{oref} \left(\frac{T}{T_{STC}} \right)^3 \cdot \exp \left(\frac{q \cdot E_g}{a \cdot K} \left(\frac{1}{T_{STC}} - \frac{1}{T} \right) \right). \quad (4)$$

Here, a_1 and a_2 are the ideality factor of diode D_1 and diode D_2 , respectively, q and K are the electron charge and Boltzmann constant, G_{STC} and T_{STC} are irradiance and temperature at standard test condition (STC) (1000 W/m², 25 °C), and E_g is the bandgap energy of the material.

Similarly, the values of R_s and R_p depending on the environmental condition are given as [5]

$$R_s = R_{sref2} (1 + K_{Rs} (T - T_{STC})) + R_{sref1} \left(\frac{G}{G_{STC}} \right)^{\gamma_{Rs}} \quad (5)$$

$$R_p = R_{pref} (1 + K_{Rp} (T - T_{STC})) \left(\frac{G}{G_{STC}} \right)^{\gamma_{Rp}}. \quad (6)$$

From (1), it is clear that the optimum values of 12p γ_{Rs} , γ_{Rp} , K_{Rs} , K_{Rp} , R_{sref1} , R_{sref2} , R_{pref} , a_1 , a_2 , I_{phref} , I_{oref} , and I_{o2ref} will provide a more accurate I - V characteristic of the solar PV. Additionally, in order to approximate the short-circuit current (I_{sc}) and open-circuit voltage (V_{oc}) at different environmental conditions, following equations are used [11]:

$$I_{sc} = (I_{scSTC} + k_i (T - T_{STC})) \frac{G}{G_{STC}}$$

$$V_{oc} = V_{ocSTC} + V_t \ln \left(\frac{G}{G_{STC}} \right) + k_v (T - T_{STC}). \quad (7)$$

It must be noted that the parameters estimated for one set of the environmental condition can predict the behavior of solar PV for all environmental conditions, which is not the case of convention models where the parameters are fixed. This is because, in the 12p-DDM, the values of I_{ph} , I_{o1} , I_{o2} , R_s , and R_p are adapted according to the variations of temperature and solar irradiance. Once the precise model of solar PV is developed, it can be used to predict the characteristic curves of solar PV at different weather conditions of a particular area. This is necessary for designing a high-efficiency inverter that is suitable for the given location [21], [22]. In addition, it can be beneficial to identify mismatch in PV array or evaluate the influence of dust in the solar PV module, by calculating the difference in real power generated by the module and predicted power by the model. This will allow performing maintenance at the right time.

III. PROBLEM FORMULATION

The diode models, discussed in the previous section, can help predict the I - V and P - V characteristics of the PV modules. For this, one needs to obtain optimized parameters of the solar PV model with negligible error. This can be done by using various optimization algorithms. In this paper, the WDO algorithm is employed and it is explained in the next section. However, as in any optimization algorithm, one has first to define the objective function that has to be minimized.

For this, the individual absolute error (IAE), which is absolute value of the difference between measured current I_m and estimated output current $I_{\text{estimated}}$, is defined first and it is given by

$$f_i(V_m, I_m, X) = \text{IAE} = \text{abs}(I_m - I_{\text{estimated}}) \quad (8)$$

where X represents the model parameters. Next, the sum of squared error (SSE) function is given by

$$\text{SSE} = \sum_{i=1}^N \text{IAE}_i^2 \quad (9)$$

where N is the number of experimental data.

Finally, the objective function is defined as the root mean square error (RMSE) value of the SSE and is given by

$$\text{RMSE} = \sqrt{\frac{1}{N} \text{SSE}}. \quad (10)$$

The objective function will aggregate the absolute error and gives the measure of predictive power. For comparison purpose, RMSE value will be normalized as

$$\text{NRMSE} = \frac{\text{RMSE}}{I_{\text{SC}_S}} 100\% \quad (11)$$

where I_{SC_S} is the short-circuit current at STC.

In most of the practical applications, the solar PV model has been used to predict the maximum power that can be extracted from the solar PV at a particular weather condition. Thus, to validate the accuracy of P - V curve of solar PV, the MAEP is calculated as

$$\text{MAEP} = \frac{\sum_{i=1}^N \text{error}_P}{N} \quad (12)$$

with

$$\text{error}_p = |P_m - P_{\text{estimated}}|. \quad (13)$$

Here, P_m is the experimentally measured power curve data and $P_{\text{estimated}}$ is the power estimated using solar PV model.

IV. WIND-DRIVEN OPTIMIZATION AND ITS IMPLEMENTATION

A. Wind-Driven Optimization Algorithm

WDO is a new nature-inspired optimization technique based on atmospheric motion [23], [17]. The WDO technique is a population-based iterative and heuristic global optimization algorithm for multidimensional problems such as the solar PV parameter optimization.

Essentially, a population of infinitesimally small air parcels navigates over an N -dimensional search space following Newton's second law of motion. The idea is based on the actual equations that describe the movement of air parcels from a high-pressure area to low-pressure area in an attempt to equalize horizontal imbalances in the air pressure. The change in pressure (P) is referred as the pressure gradient. Newton's second law states that total force (F_t) applied on air parcel causes the air parcel to accelerate with an acceleration a in the same direction of the force

$$\rho \cdot \vec{a} = \sum \vec{F}_t. \quad (14)$$

The four forces that affect the movement of air parcel are pressure gradient force (F_{PG}), frictional force (F_F), gravitational force (F_G) and Coriolis force (F_C). By assuming air has finite volume (δV), the force because of pressure gradient can be expressed as

$$\vec{F}_{\text{PG}} = -\vec{\nabla}P \cdot \delta V. \quad (15)$$

The frictional force opposes the air parcel motion started by F_{PG} , and can be expressed in a simplified form as [17]

$$\vec{F}_F = -\rho \alpha \vec{u}. \quad (16)$$

Here, ρ is the air density of a small air parcel, α is the frictional coefficient, and \vec{u} is the wind velocity vector.

The gravitational force pulls the air parcel to the center of the earth that causes a vertical motion defined as

$$\vec{F}_G = \rho \cdot \delta V \cdot \vec{g} \quad (17)$$

with \vec{g} being the gravitation vector.

The rotation of the earth causes deflection in the motion of air parcel and named as Coriolis force. This force will work in such a way that velocity in one direction is influenced by velocity of another direction. It can be expressed as

$$\vec{F}_C = -2\theta \times \vec{u} \quad (18)$$

where θ represents the rotation of earth.

Therefore, including F_{PG} , F_F , F_G , and F_C in total force described in (14) can be rewritten as

$$\rho \cdot \frac{\Delta \vec{u}}{\Delta t} = \rho \cdot \delta V \cdot \vec{g} - \vec{\nabla}P \cdot \delta V - \rho \alpha \vec{u} - 2\theta \times \vec{u}. \quad (19)$$

Since air parcels are infinitesimal and dimensionless, δV can be neglected from (19). In order to make the equation simpler, Δt is assumed to be equal to 1. Substituting the ideal gas equation in (19) and rewriting ρ in terms of the current pressure P_c , temperature T , and universal gas constant R , we get

$$\vec{\Delta u} = \vec{g} + \left(-\vec{\nabla}P \cdot \frac{RT}{P_c} \right) + (-\alpha \vec{u}) - \left(\frac{2\theta \vec{u} RT}{P_c} \right). \quad (20)$$

In (20), the first and the second vectors do not depend on position (y) or velocity (u), therefore both the vectors are broken down into their magnitude and direction.

Since gravitational force always try to move toward the zeroth position, it can be rewritten as $|g|(0 - y_c)$, where y_c is current position of the the air parcel. Similarly, since the pressure gradient move toward the optimal solution, therefore it can be rewritten as $|\nabla P|(y_{opt} - y_c)$. Moreover, the velocity equation depends on its pressure value. Therefore, if the pressure increases the velocity gets updated incorrectly. In order to cater for that, (20) is modified based on the rank of the pressure. After every iteration, the air parcels are ranked in descending order based on their pressure values. If r is the rank of the air parcel, the new velocity and position in j th dimension of k th air parcel will be updated according to

$$\begin{aligned} \vec{u}_{new_j}^k &= (1 - \alpha) \vec{u}_{c_j}^k - g y_{c_j}^k + \left(\left| 1 - \frac{1}{r^k} \right| \right. \\ &\quad \left. \cdot \left(y_{opt_j}^k - y_{c_j}^k \right) RT \right) + \left(\frac{c \cdot \vec{u}_0}{r^k} \right) \end{aligned} \quad (21)$$

$$\vec{y}_{new_j}^k = \vec{y}_{c_j}^k + \left(\vec{u}_{new_j}^k \times \Delta t \right). \quad (22)$$

Here, \vec{u}_{new} stands for the velocity of the next iteration, \vec{u}_c is the velocity of the current iteration, y_{opt} is the optimal position, $c = -2RT$, and $\vec{u}_0 = \theta \times \vec{u}$. For each dimension, the WDO allows air parcel to travel in a boundary of $[-1, 1]$. To obtain the optimized objective function value, the coefficients α , g , RT , and c in (21) play an important role. In order to find the optimized values of these constants, CMAES technique is used. It does not require any inputs other than population size [17]. Since WDO uses simple steps to reach the optimized values, it is a desirable technique for optimizing the nonlinear problems. This technique is proper for parameter estimation because it explores and continuously exploits the parameters. The main feature of the technique is that compared with other nature-inspired algorithms, WDO introduces gravitational and Coriolis forces in the velocity updating equation. In other algorithms, candidates of the population may fly out or stuck at the boundaries of each dimension, therefore this holds back the algorithm for productively exploring the entire search space. In WDO, the gravitational force pulls the air parcels back to the search space if they remain stuck. Thus, it prevents local convergence of the parameters by always jumping to a new position in search of the low-pressure area. Additionally, in other algorithms, the dimensions of a candidate are influenced by the same dimension of other population (global best). However, in WDO by Coriolis force, each dimension is randomly affected by the other dimensions. This improves the robustness in the motion of air parcels and allows an extra degree of freedom for fine tuning. Both these properties are not introduced in any other algorithms.

B. Wind-Driven Optimization Implemented for Parameter Estimation of Solar Photovoltaic

The implementation of WDO for parameter estimation is shown as a flowchart in Fig. 2. As can be seen from the flowchart, it involves different steps that are explained as follows.

Step 1: Initialization of parameters: Population size (number of air parcels) = N_k , maximum number of iterations =

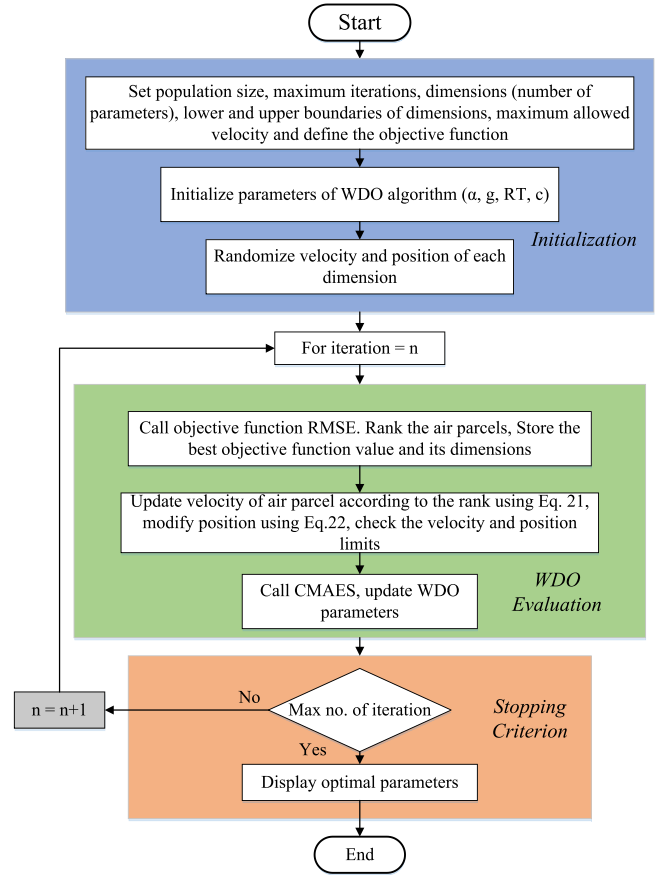


Fig. 2. Flowchart of WDO algorithm.

N_i , dimensions of air parcel (number of parameters) = N_j , and dimension limits (Max_j and Min_j) and maximum velocity u_{max} are initialized. Define the objective function (10). Randomly generate the velocity $(u_1^k, u_2^k, \dots, u_{N_j}^k)$ and position $(y_1^k, y_2^k, \dots, y_{N_j}^k)$ for each air parcels. CMAES generates the predetermined coefficients.

Step 2: Pressure evaluation: In this step, the pressure of each air parcel is evaluated by the objective function (10). The parameter limits are mapped from $[-1, 1]$ to the actual values as

$$x_j^k = (Max_j - Min_j) \times \left(\left(\frac{y_j^k + 1}{2} \right) + Min_j \right). \quad (23)$$

Step 3: Ranking of air parcel: According to the descending order of pressure value, air parcels are ranked.

Step 4: Updating: CMAES will generate a new set of coefficients. On the basis of the rank of the air parcel, velocity and position of each air parcel are updated using (21) and (22). In order to preclude air parcel in taking large steps, air parcels are limited to maximum velocity. If $u_{new_j}^p$ is above or below the u_{max} , velocity will be updated in such a way that

$$u_{new_j}^p = \begin{cases} u_{max} & \text{if } u_{new_j}^k > u_{max} \\ -u_{max} & \text{if } u_{new_j}^k < -u_{max} \end{cases}.$$

Here, the magnitude of the velocity is limited, while the direction is maintained the same.

TABLE I
ESTIMATED PARAMETERS OF 12P-DD MODEL OF KC200GT 215 MODULE

| Parameters | Values | B [4] | C [21] | D [30] | E [31] | F [32] |
|--------------------------|--------|-------|--------|--------|--------|--------|
| a_1 | 1.2506 | 1 | 1 | 1.2844 | 1 | 1.28 |
| a_2 | 2.751 | | 2 | | 1.2 | |
| R_S (m Ω) | 9.3 | 271 | 379.5 | 236 | 303 | 230 |
| R_P (Ω) | 250 | 171.2 | 278.91 | 524.2 | 343.1 | 405.2 |
| I_{ph} (A) | 8.1192 | 8.193 | 8.219 | 8.213 | 8.21 | 8.214 |
| I_{o1} (nA) | 72.73 | 0.3 | 0.3795 | 78.4 | 11.1 | 75.01 |
| I_{o2} (nA) | 1151.2 | | 4433.4 | | 11.1 | |
| γ_{R_s} | -0.063 | NA | NA | NA | NA | NA |
| γ_{R_p} | -0.862 | NA | NA | NA | NA | NA |
| K_{R_s} | 0.0033 | NA | NA | NA | NA | NA |
| K_{R_p} | -0.002 | NA | NA | NA | NA | NA |
| R_{sref1} (Ω) | 0.0047 | NA | NA | NA | NA | NA |
| R_{sref2} (Ω) | 0.0047 | NA | NA | NA | NA | NA |
| R_{pref} (Ω) | 250 | NA | NA | NA | NA | NA |
| I_{phref} (A) | 8.1192 | NA | NA | NA | NA | NA |
| I_{o1ref} (nA) | 72.73 | NA | NA | NA | NA | NA |
| I_{o2ref} (nA) | 1151.2 | NA | NA | NA | NA | NA |
| MAEP (W) | 0.3594 | 0.499 | 1.1328 | 1.337 | 0.92 | 1.258 |
| NRMSE (%) | 0.3846 | 0.515 | 1.1675 | 1.3733 | 1.007 | 1.298 |

Step 5: Termination criterion: Until the maximum number of iteration reached, steps 2–4 are repeated. Finally, the best pressure position is recorded as the optimized result.

V. RESULTS AND DISCUSSION

A. Comparison With Experimental Curves at the Controlled Environmental Condition

1) *Experimental Data of Kyocera – KC200GT 215:* The 12p of solar PV model described previously are first coded in MATLAB/Simulink and are used to test the proposed optimization algorithm. The 25 set experimental data of multicrystal PV module Kyocera – KC200GT 215 provided in [24] is used to find the objective function. The dimensions γ_{R_s} , γ_{R_p} , K_{R_s} , K_{R_p} , R_{sref1} , R_{sref2} , R_{pref} , a_1 , a_2 , I_{phref} , I_{o1ref} , and I_{o2ref} have been assigned a boundary limit between $(-5$ to $-0.05)$, $(-5$ to $-0.05)$, $(0.001$ to $0.01)$, $(-0.01$ to $-0.001)$, $(0.01$ to $3 \Omega)$, $(0.01$ to $3 \Omega)$, $(500$ to $2000 \Omega)$, $(1$ to $3)$, $(1$ to $3)$, $(0$ to 10 A), $(0$ to 1 A), and $(0$ to 1 A), respectively.

Table I presents the comparison of the proposed technique with the techniques already available in the literature. The comparison was done based on two performance indexes such as MAEP and NRMSE. All the parameters were estimated at the STC. Table I clearly exhibits that the 12p-DDM using WDO shows better results for both performance indexes MAEP and NRMSE. This clearly reveals that WDO algorithm performs well in terms of accuracy.

Moreover, the 12p-DDM with WDO technique require only one set of parameters for all environmental conditions. This can be substantiated by analyzing the average MEAP and NRMSE for seven set of environmental conditions. The values of $MEAP_{avg}$ and $NRMSE_{avg}$ are obtained as

$$MEAP_{avg} = 0.55 \text{ W}, \quad NRMSE_{avg} = 0.436\%.$$

Fig. 3(a) and (b) shows the comparison of I – V and P – V graph obtained experimentally and using the proposed method

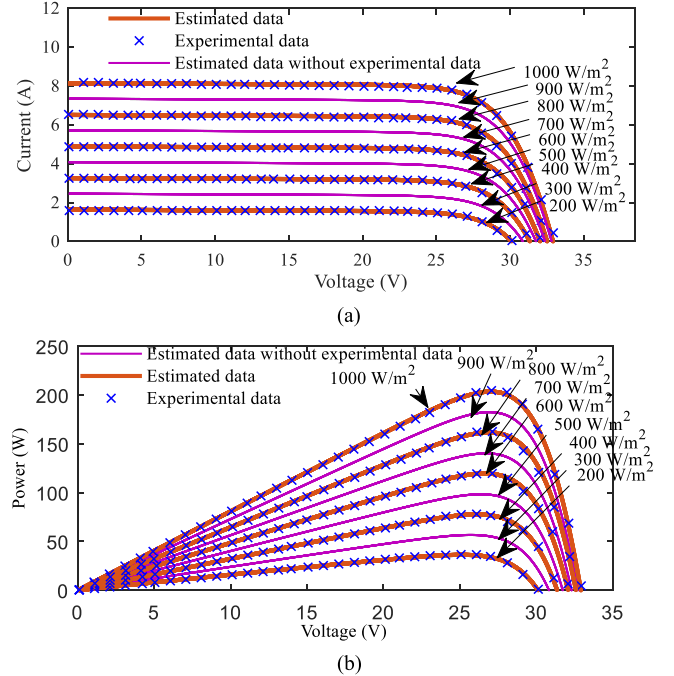


Fig. 3. KC200GT 215. (a) I – V characteristics at different irradiance. (b) P – V characteristic curve of KC200GT 215 at different irradiance.

at different irradiance. This visualize that 12p-DDM with WDO technique exactly replicate the experimental curves at different environmental conditions. Moreover, from Fig. 3, estimated data without experimental data curves ensure that the 12p-DDM could estimate the PV characteristics for all environmental conditions. It must be noted that the same set of estimated parameters are used for all environmental conditions. It proves that Kyocera – KC200GT 215 can be exactly modeled using 12p-DDM using the parameters as mentioned in Table I.

2) *Experimental Data of RTC France Solar Cell:* In order to verify 12p-DDM with WDO technique as a reliable alternative in modeling the solar PV, the results obtained are compared with the results presented in the recent literature. The experimental data of 57-mm-diameter RTC France silicon solar cell at 1000 W/m^2 irradiance and 33°C temperature presented in [25] are used for the comparison. This particular solar cell was chosen because, in much recent literature, this experimental data had been used as comparative platform of the obtained results. The comparison of results estimated by WDO and other techniques such as bee pollinator flower pollination algorithm (BPFPA) [26], self-adaptive teaching learning based optimization [27], cat swarm optimization [28], chaotic whale optimization algorithm (CWOA) [29], and FPA [15] has been shown in Table II.

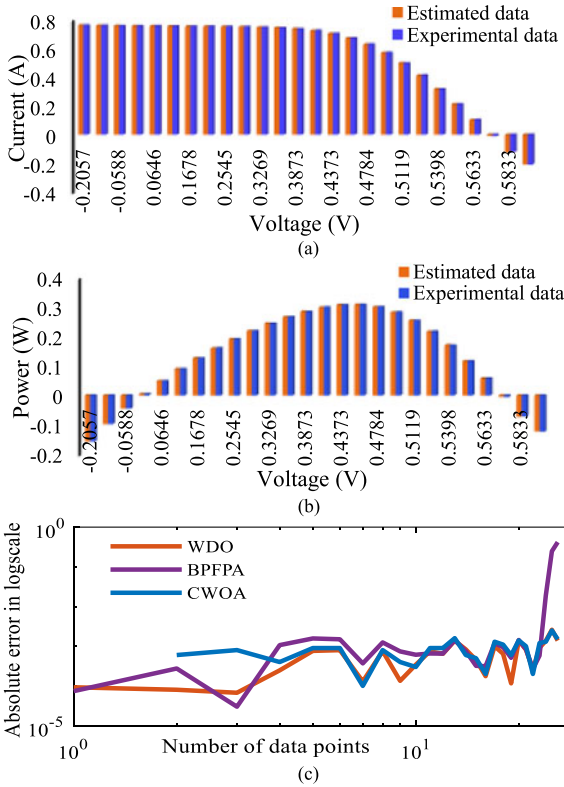
From Table II, it is significant that the MAEP and NRMSE values of the proposed method outperform (0.357 mW and 0.127%) among the methods considered for comparison. Fig. 4(a) and (b) shows the I – V and P – V curve of the solar cell. This clearly supports the results shown in Table II, the estimated curve exactly matches the experimental curve with negligible error. Fig. 4(c) shows the comparison of absolute error curve of WDO, BPFPA, and CWOA. WDO shows better result compared with the other two techniques because of the following reasons:

TABLE II
 COMPARISON OF WDO PERFORMANCE WITH OTHER ALGORITHMS

| Parameter | WDO | B [26] | C [27] | D [28] | E [29] | F [15] |
|--------------------------|--------|--------|--------|--------|--------|--------|
| a_1 | 2.3776 | 1.479 | 1.4598 | 1.4515 | 1.4565 | 1.4747 |
| a_2 | 1.4604 | 2.00 | 1.999 | 1.997 | 1.9899 | 2 |
| R_S (m Ω) | 36.7 | 36.4 | 36.63 | 36.73 | 36.66 | 36.3 |
| R_P (Ω) | 53.245 | 59.62 | 55.117 | 55.381 | 55.201 | 52.347 |
| I_{ph} (A) | 0.7609 | 0.76 | 0.7607 | 0.7607 | 0.7607 | 0.7607 |
| I_{o1} (μ A) | 1.4661 | 0.321 | 0.2509 | 0.2273 | 0.2415 | 0.3 |
| I_{o2} (μ A) | 0.0257 | 0.045 | 0.5454 | 0.7279 | 0.600 | 0.1661 |
| γ_{Rs} | -3.066 | NA | NA | NA | NA | NA |
| γ_{Rp} | -4.998 | NA | NA | NA | NA | NA |
| K_{Rs} | 0.0081 | NA | NA | NA | NA | NA |
| K_{Rp} | -0.001 | NA | NA | NA | NA | NA |
| R_{sref1} (Ω) | 0.0178 | NA | NA | NA | NA | NA |
| R_{sref2} (Ω) | 0.0178 | NA | NA | NA | NA | NA |
| R_{pref} (Ω) | 53.762 | NA | NA | NA | NA | NA |
| I_{phref} (A) | 0.7248 | NA | NA | NA | NA | NA |
| I_{o1ref} (μ A) | 0.8599 | NA | NA | NA | NA | NA |
| I_{o2ref} (μ A) | 0.0113 | NA | NA | NA | NA | NA |
| MAEP (mW) | 0.357 | 2.2 | 0.361 | 0.359 | 0.3872 | 0.45 |
| NRMSE (%) | 0.127 | 0.8438 | 0.1335 | 0.1328 | 0.1627 | 0.182 |

 TABLE III
 12p-DD MODEL PARAMETERS FOR DIFFERENT SOLAR PV MODULES

| Parameters | Shell, SP140-PC | KYOCERA KS20T | Sunmodule SW245 poly | Solo Panel SP190 |
|--------------------------|-----------------|---------------|----------------------|------------------|
| a_1 | 1.9618 | 2.1264 | 4.1710 | 1.5441 |
| a_2 | 1.3609 | 1.2656 | 1.518 | 1.5373 |
| R_S (m Ω) | 440 | 90 | 5.8 | 19.5 |
| R_P (Ω) | 1148.6 | 1329.1 | 799.7526 | 40.0909 |
| I_{ph} (A) | 4.6994 | 1.263 | 8.4901 | 4.3021 |
| I_{o1} (μ A) | 1.3858 | 4.226 | 0.03737 | 1.4714 |
| I_{o2} (μ A) | 1.3334 | 0.01 | 0.92614 | 1.0279 |
| γ_{Rs} | -3.1913 | -0.9137 | -0.0504 | -1.7493 |
| γ_{Rp} | -4.6804 | -0.4239 | -0.1763 | -2.9702 |
| K_{Rs} | 0.0069 | 0.01 | 0.0073 | 0.0068 |
| K_{Rp} | -0.001 | -0.0038 | -0.0051 | -0.0066 |
| R_{sref1} (Ω) | 0.0022 | 0.0045 | 0.023 | 0.0098 |
| R_{sref2} (Ω) | 0.0022 | 0.0045 | 0.023 | 0.0098 |
| R_{pref} (Ω) | 1500 | 1329.1 | 799.7526 | 40.0909 |
| I_{phref} (A) | 4.6967 | 1.263 | 8.4901 | 4.3021 |
| I_{o1ref} (μ A) | 0.013393 | 4.2226 | 0.03737 | 1.4714 |
| I_{o2ref} (μ A) | 1.2609 | 0.01 | 0.92614 | 1.0279 |
| MAEP (W) | 0.0063 | 0.009 | 0.0054 | 0.0016 |
| NRMSE (%) | 0.1264 | 0.442 | 0.08165 | 0.088 |


 Fig. 4. RTC France solar cell. (a) I - V characteristics. (b) P - V characteristics. (c) Absolute error of three optimization techniques.

In CWOA technique, position updating is based on the chaotic sequence, which is very sensitive to the primary solution [29]. Therefore, this makes the control variable jumps to the global solution. Even although this exploration in parameters creates scattering, but because of the absence of exploitation in parameters, CWOA becomes less diverse and produces an error. BPFPA shows both exploration and exploitation of parameters but it stops searching for diverse solution once it converges to an optimal region [26]. Because of that, all the parameters may

not converge to the global optimum. Therefore, the diversity in solution is less in BPFPA that create error values. By utilizing the gravitational and Coriolis forces in the updating velocity, both exploration and exploitation of parameters are available in WDO; in addition to that, it always establishes randomness that converges all parameters to the optimum value.

B. Comparison With Datasheet Curve

In this section, the flexibility of the 12p-DDM of the solar PV with WDO is validated. In order to verify that, the characteristic curves estimated by WDO are compared with the data sheet characteristic curves of different solar PV modules such as Shell SP140-PC (monocrystalline) [33], KYOCERA KS20T (multicrystal) [34], Sunmodule SW245 poly (polycrystalline) [35], and Solo panel SP190 (thin film) [36]. The data in datasheet curve obtained using a curve extractor algorithm developed in MATLAB. The boundaries assigned to all the PV modules parameters are $\gamma_{Rs} \in [-5, -2]$, $\gamma_{Rp} \in [-5, -0.05]$, $K_{Rs} \in [0.001, 0.01]$, $K_{Rp} \in [-0.01, -0.001]$, $R_{sref1} \in [0.001, 1]\Omega$, $R_{sref2} \in [0.001, 1]\Omega$, $R_{pref} \in [50, 2000]\Omega$, $a_1, a_2 \in [1, 5]$, $I_{phref} \in [0.1, 10]A$, and $I_{o1ref}, I_{o2ref} \in [0.1, 5]\mu A$.

Table III shows the parameter values of all the modules under STC. The MAEP and NRMSE of each module given in Table III substantiate that the proposed model can be used to predict the I - V and P - V characteristics of different solar PV technologies very precisely.

C. Comparison With an Experimental Curve at Uncontrolled Environmental Conditions

The proposed method can also be effectively used for uncontrolled environmental conditions varying irradiation and temperature. In order to authenticate the 12p-DDM of the solar PV,

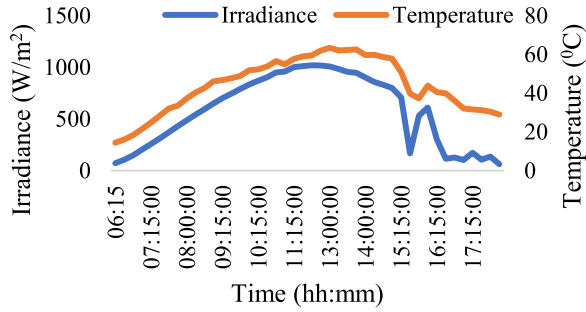


Fig. 5. Environmental factors in Golden, CO, USA, provided by NREL.

TABLE IV
12P-DD MODEL PARAMETERS OF A-SI TANDEM MODULE

| Parameters | Values |
|--------------------------|----------|
| a_1 | 2.1737 |
| a_2 | 2.6358 |
| R_S (Ω) | 1.2858 |
| R_P (Ω) | 558.3285 |
| I_{ph} (A) | 1.1717 |
| I_{o1} (μ A) | 0.22439 |
| I_{o2} (μ A) | 6.1244 |
| γ_{R_s} | -3.7619 |
| γ_{R_p} | -5.7491 |
| K_{R_s} | 0.0072 |
| K_{R_p} | -0.0031 |
| R_{sref1} (Ω) | 0.5884 |
| R_{sref2} (Ω) | 0.5884 |
| R_{pref} (Ω) | 615.9002 |
| I_{phref} (A) | 1.1271 |
| I_{o1ref} (μ A) | 52.659 |
| I_{o2ref} (μ A) | 2.0135 |
| MAEP (W) | 0.168 |
| NRMSE (%) | 0.7855 |

the obtained results are compared with the experimental curve. The real-time data are obtained from National Renewable Energy Laboratory (NREL), which includes the $I-V$ curve data of a day for the location Golden, CO, USA. NREL used amorphous silicon (a-Si) tandem junction (aSi Tandem 90–31) solar PV module for the experiment. The plane of array irradiance was measured using Kipp and Zonen CMP22 pyranometer and PV modules back surface temperature was measured using Omega Model Col-T style 1 thermocouple. The PV module tilt angle is 40° and the horizontal angle is 180° . The data were measured at every 15 min interval from 06:00 A.M. to 06:00 P.M. The irradiance and temperature variations are shown in Fig. 5. The solar PV operates at the maximum power point region. To find the parameters of 12p-DD solar PV module, a set of data was measured at the reference irradiance (1012 W/m^2) and temperature (57.7°C). The optimized values of the parameters are shown in Table IV. Fig. 6 shows that the estimated curve exactly agrees with the measured curve. Hence, it validates that the 12p-DDM with these parameters can show similar characteristics as aSi Tandem 90-31 solar PV module. Once the validation has been completed, this model can be used to predict the output of the solar PV. In order to authenticate that, the varying irradiance and temperature, as shown in Fig. 5, has been used for the prediction of power from the module. Fig. 7 shows that the proposed method exactly predicts the characteristics of solar PV module

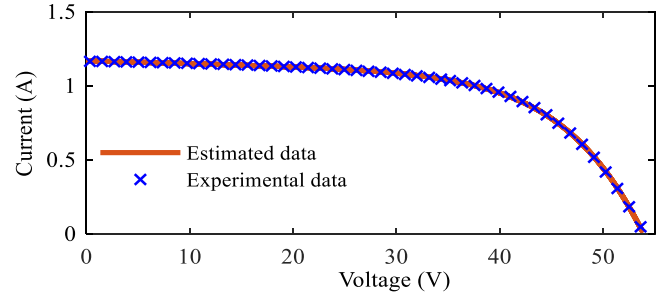


Fig. 6. $I-V$ characteristics of a-Si Tandem module at 1012 W/m^2 and 57.7°C .

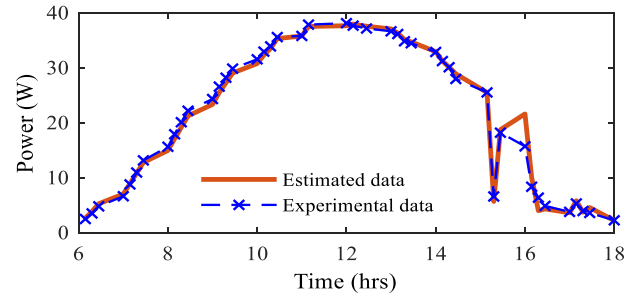


Fig. 7. Comparison of actual and predicted power at different environmental conditions.

at different varying environmental conditions. Meanwhile, the Table IV shows that the two performance indexes MAEP and NRMSE of 12p-DDM are low. This validates that the proposed method can be exactly used to model the solar PV for computer simulation to predict the characteristics of the module for any environmental conditions.

VI. CONCLUSION

In this paper, the effectiveness of the WDO algorithm for parameter estimation of a 12p-DDM of solar PV is shown. The validation of the proposed algorithm was performed by comparing the results obtained to three different sets of data, namely the following:

- 1) experimental data at the controlled environmental condition;
- 2) data sheet curves provided by the manufacturers; and
- 3) real-time experimental data at the uncontrolled environmental condition.

Additionally, in order to claim the results obtained by the WDO algorithm shows better accuracy, it is compared with several parameter estimation techniques available literature. It was noticed that the WDO algorithm attains very low MAEP and NRMSE values for all types of solar PV (KC200GT 215, RTC France, SP140PC, KS20T, SP190, SW245poly and a-si Tandem 90-31). Meanwhile, all the $I-V$ and $P-V$ characteristic curves demonstrate that the estimated curve exactly matches the measured curve with negligible errors. In addition to that, the algorithm is very simple and easy to use.

As a general conclusion, the WDO algorithm can be recommended as the accurate and flexible optimization algorithm for parameter estimation of solar PV model.

ACKNOWLEDGMENT

The authors would like to thank W. Marion (Principal Engineer, NREL) for providing necessary real-time data of the solar PV module.

REFERENCES

- [1] P. Bharadwaj, K. N. Chaudhury, and V. John, "Sequential optimization for PV panel parameter estimation," *IEEE J. Photovolt.*, vol. 6, no. 5, pp. 1261–1268, Sep. 2016.
- [2] S. Shongwe and M. Hanif, "Comparative analysis of different single-diode PV modeling methods," *IEEE J. Photovolt.*, vol. 5, no. 3, pp. 938–946, May 2015.
- [3] K. Rühle, M. K. Juhl, M. D. Abbott, and M. Kasemann, "Evaluating crystalline silicon solar cells at low light intensities using intensity-dependent analysis of I–V parameters," *IEEE J. Photovolt.*, vol. 5, no. 3, pp. 926–931, May 2015.
- [4] E. A. Silva, F. Bradascchia, M. C. Cavalcanti, and A. J. Nascimento, "Parameter estimation method to improve the accuracy of the photovoltaic electrical model," *IEEE J. Photovolt.*, vol. 6, no. 1, pp. 278–285, Jan. 2016.
- [5] E. A. Silva *et al.*, "An eight-parameter adaptive model for the single diode equivalent circuit based on the photovoltaic module's physics," *IEEE J. Photovolt.*, vol. 7, no. 4, pp. 1115–1123, Jul. 2017.
- [6] D. S. Chan and J. C. Phang, "Analytical methods for the extraction of solar-cell single-and double-diode model parameters from IV characteristics," *IEEE Trans. Electron Devices*, vol. ED-34, no. 2, pp. 286–293, Feb. 1987.
- [7] G. Farivar, B. Asaei, and S. Mehrnami, "An analytical solution for tracking photovoltaic module MPP," *IEEE J. Photovolt.*, vol. 3, no. 3, pp. 1053–1061, Jul. 2013.
- [8] M. S. Ismail, M. Moghavvemi, and T. M. I. Mahila, "Characterization of PV panel and global optimization of its model parameter using genetic algorithm," *Energy Convers. Manage.*, vol. 73, pp. 10–25, Sep. 2013.
- [9] M. Derick, C. Rani, M. Rajesh, K. Busawon, and R. Binns, "Estimation of solar photovoltaic parameters using pattern search algorithm," in *International Conference on Emerging Trends in Electrical, Electronic and Communications Engineering*. Cham, Switzerland: Springer, Nov. 2016.
- [10] B. Jacob, K. Balasubramanian, S. M. Azharuddin, and N. Rajasekar, "Solar PV modelling and parameter extraction using artificial immune system," *Energy Procedia*, vol. 1, no. 75, pp. 331–336, Aug. 2015.
- [11] N. Rajasekar, N. Krishna Kumar, and R. Venugopalan, "Bacterial foraging algorithm based PV parameter estimation," *Sol. Energy*, vol. 97, pp. 255–265, Nov. 2013.
- [12] K. M. El-Naggar, M. R. Al Rashidi, M. F. Al Hajri, and A. K. Al-Othman, "Simulated annealing algorithm for photovoltaic parameter identification," *Sol. Energy*, vol. 86, no. 1, pp. 266–274, Jan. 2012.
- [13] A. Alireza and A. Rezazadeh, "Parameter identification for solar cell models using harmony search-based algorithms," *Sol. Energy*, vol. 86, no. 11, pp. 3241–3249, Nov. 2012.
- [14] D. Oliva, E. Cuevas, and G. Pajares, "Parameter identification of solar cells using artificial bee colony optimization," *Energy*, vol. 72, pp. 93–102, Aug. 2014.
- [15] D. F. Alam, D. A. Youstri, and M. B. Eteiba, "Flower pollination algorithm based solar PV parameter estimation," *Energy Convers. Manage.*, vol. 101, pp. 410–422, Sep. 2015.
- [16] J. Ma *et al.*, "Parameter estimation of photovoltaic models via cuckoo search," *J. Appl. Math.*, vol. 7, pp. 1–8, Aug. 2013.
- [17] Z. Bayraktar, M. Komurcu, J. A. Bossard, and D. H. Werner, "The wind driven optimization technique and its application in electromagnetics," *IEEE Trans. Antennas Propag.*, vol. 61, no. 5, pp. 2745–2757, May 2013.
- [18] A. K. Bhandari, V. K. Singh, A. Kumar, and G. K. Singh, "Cuckoo search algorithm and wind driven optimization based study of satellite image segmentation for multilevel thresholding using Kapur's entropy," *Expert Syst. Appl.*, vol. 41, no. 7, pp. 3538–3560, Jun. 2014.
- [19] S. Kolesnik *et al.*, "Solar irradiation independent expression for photovoltaic generator maximum power line," *IEEE J. Photovolt.*, vol. 7, no. 5, pp. 1416–1420, Sep. 2017.
- [20] M. Derick *et al.*, "An improved optimization technique for estimation of solar photovoltaic parameters," *Sol. Energy*, vol. 15, no. 157, pp. 116–124, Nov. 2017.
- [21] M. Hejri, H. Mokhtari, M. R. Azizian, M. Ghandhari, and L. Soder, "On the parameter extraction of a five-parameter double-diode model of photovoltaic cells and modules," *IEEE J. Photovolt.*, vol. 4, no. 3, pp. 915–923, May 2014.

- [22] B. C. Babu and S. Gurjar, "A novel simplified two-diode model of photovoltaic (PV) module," *IEEE J. Photovolt.*, vol. 4, no. 4, pp. 1156–1161, Jul. 2014.
- [23] Z. Bayraktar, "Novel meta-surface design synthesis via nature-inspired optimization algorithms," Ph.D. dissertation, Pennsylvania State Univ., State College, PA, USA, 2011.
- [24] C. Pauls, "Optimization approaches for parameter estimation and maximum power point tracking (MPPT) of photovoltaic systems," Ph.D. dissertation, Univ. Liverpool, Liverpool, U.K., 2014.
- [25] T. Easwarakhanthan, J. Bottin, I. Bouhouch, and C. Boutrit, "Nonlinear minimization algorithm for determining the solar cell parameters with microcomputers," *Int. J. Sol. Energy*, vol. 4, no. 1, pp. 1–12, Jan. 1986.
- [26] J. P. Ram, T. S. Babu, T. Dragicicvic, and N. Rajasekar, "A new hybrid bee pollinator flower pollination algorithm for solar PV parameter estimation," *Energy Convers. Manage.*, vol. 135, pp. 463–476, Mar. 2017.
- [27] K. Yu, X. Chen, X. Wang, and Z. Wang, "Parameters identification of photovoltaic models using self-adaptive teaching-learning-based optimization," *Energy Convers. Manage.*, vol. 145, pp. 233–246, Aug. 2017.
- [28] L. Guo, Z. Meng, Y. Sun, and L. Wang, "Parameter identification and sensitivity analysis of solar cell models with cat swarm optimization algorithm," *Energy Convers. Manage.*, vol. 108, pp. 520–528, Jan. 2016.
- [29] D. Oliva, M. A. El Aziz, and A. E. Hassanien, "Parameter estimation of photovoltaic cells using an improved chaotic whale optimization algorithm," *Appl. Energy*, vol. 200, pp. 141–154, Aug. 2017.
- [30] E. Moshksar and T. Ghanbari, "Adaptive estimation approach for parameter identification of photovoltaic modules," *IEEE J. Photovolt.*, vol. 7, no. 2, pp. 614–623, Mar. 2017.
- [31] T. S. Babu, J. P. Ram, K. Sangeetha, A. Laudani, and N. Rajasekar, "Parameter extraction of two diode solar PV model using Fireworks algorithm," *Sol. Energy*, vol. 15, no. 140, pp. 265–276, Dec. 2016.
- [32] H. M. Hasanien, "Shuffled frog leaping algorithm for photovoltaic model identification," *IEEE Trans. Sustain. Energy*, vol. 6, no. 2, pp. 509–515, Apr. 2015.
- [33] Shell solar SP140-PC monocrystalline PV module, M55 photovoltaic solar module. [Online]. Available: <http://abcsolar.com/pdf/sp140pc.pdf>. Accessed on: Jul. 3, 2017.
- [34] Kyocera-KS20T multi-crystal PV module. [Online]. Available: <https://www.kyocerasolar.com/dealers/product-center/archives/spec-sheets/Solartec-KS20.pdf>. Accessed on: Jul. 3, 2017.
- [35] Sunmodule SW245 poly PV module. [Online]. Available: <http://la.solarworld.com/~media/www/files/datasheets/sunmodule-poly/sunmodule-solar-panel-245-poly-ds.pdf>. Accessed on: Jul. 3, 2017.
- [36] Solo panel SP190 thin film PV module. [Online]. Available: <http://solopower.com/wpcontent/uploads/DataSheetSolopanelSP1-02042016.pdf>. Accessed on: Nov. 15, 2017.



Mathew Derick received the B.Tech. degree in electrical and electronics engineering from Kannur University, Kannur, India, in 2011, and the M.Tech. degree in power electronics and drives from Karunya University, Coimbatore, India, in 2014. He is currently working toward the Ph.D. degree with the School of Electrical Engineering, VIT University, Vellore, India.

He is working on modeling of solar PV to design inverter for grid connected application.



Chinnappa Rani (SM'16) received the B.Eng. (first class) and M.Tech. degrees from VIT University, Vellore, India, in 1998 and 2006, respectively, and the Ph.D. degree from Northumbria University, Newcastle upon Tyne, U.K., in 2014, all in electrical engineering.

After that, she joined the Northumbria Photovoltaic Applications Centre, Northumbria University, as a Postdoctoral Researcher. She is currently an Associate Professor at VIT University. She leads an appreciable number of research groups and projects in

the areas such as solar photovoltaic, wind energy, power generation dispatch, power system optimization, and artificial intelligence techniques.



Muthu Rajesh Kumar (SM'16) received the B.E. degree in electronics and communication engineering from Madras University, Chennai, India, in 2000, the M.E. degree in electrical drives and embedded control from the College of Engineering, Anna University, Chennai, India, in 2005, and the M.B.A. degree in systems from Alagappa University, Karaikudi, India, in 2008.

Since 2000, he has been in teaching with the Department of Electronics and Communication Engineering (India) and Faculty of Engineering and Environment (U.K.). He is currently an Associate Professor with the School of Electronics Engineering, VIT University, Vellore, India. His research interests include image engineering and security, biometrics, image/video watermarking and cryptography, perceptual hashing, pattern recognition, and optimization technique.

Mr. Rajesh Kumar is a Chartered Engineer (with a membership of the IET, U.K.). He was the recipient of the Research Scholarships award for his Ph.D. from Northumbria University, Newcastle upon Tyne, U.K., in 2016.



Yue Wang received the B.Eng. and Ph.D. degrees in electronic and electrical engineering from the University of Strathclyde, Glasgow, U.K., in 2010 and 2014, respectively.

She is currently a Research Fellow at Northumbria University, Newcastle upon Tyne, U.K. Her research interests include smart integration of electric vehicles and renewable energy into power systems and wind turbine condition monitoring.



Richard Binns received the Graduate degree in electronic and information engineering from Huddersfield University, Huddersfield, U.K., in 1993, and the Ph.D. degree in analogue test strategies from Huddersfield University, Huddersfield, U.K., in 1997.

He is the Head of Department of Mathematics Physics and Electrical Engineering, Northumbria University, Newcastle upon Tyne, U.K. He is currently responsible for a department of 50 staff members of the faculty executive routinely headed up professional body accreditations and establishing collaborative links to institutions in Malaysia, Singapore, and China. He moved to Northumbria University in 2001 on an EPSRC postdoctoral contract looking into analogue synthesis tool development in collaboration with Ericson Components and Cadence Design Systems. His research interests include design of electronics for visible light communications, energy management in electric vehicles, research into radiation detection mechanisms for personal dosimetry, and power control systems development.



Krishna Busawon (SM'15) received the first degree in mathematics from the University of St-Etienne, St-Etienne, France, in 1989 and the B.Sc., and M.Sc. degrees in electrical engineering in 1990 and 1991, respectively, and Ph.D. degree in control system from the University of Lyon I, Lyon, France, in 1996.

He is a Professor of control systems engineering and is currently the Head of Nonlinear Control Research Group, Faculty of Engineering and Environment. His research interests include mathematical modeling, optimization, nonlinear control and observer design, and fault detection and isolation with application to various engineering disciplines such as mechanical, power, and biotechnological systems. He has authored or coauthored more than 150 research papers in these areas.